

Parameter estimation of flow-measurement in digital angiography

Krisztian Veress
Institute of Informatics
University of Szeged, Szeged, Hungary
verkri@inf.u-szeged.hu

Csendes Tibor
Institute of Informatics
University of Szeged, Szeged, Hungary
csendes@inf.u-szeged.hu

Abstract

The purpose of angiographic procedures used in cardiovascular interventions is to classify the patient's potential of regeneration after strokes caused by dead blood cells in the main arteria. The flow of blood into heart's capillaries is measured using x-ray radiometry with contrastive fluids.

Our task was to fit a 5-parameter Gamma function to the intensity samples extracted from the x-ray angiograms. The estimation of this function's parameters is hard given that the raw data set is heavily polluted with several different types of noise.

Our complete solution has four main parts which have also been successfully verified and validated. First, we propose a solution for eliminating the noise by applying a specially designed moving window Gauss filter. Secondly, we have designed an algorithm for computing a good initial guess for the Levenberg-Marquardt optimizer in order to achieve the required precision. Third, an algorithm is proposed for selecting significant points on the smoothed data set with an interval-based classification method. Finally we apply the LM algorithm to compute the solutions in a non-linear least squares way.

We have also designed an algorithm which can be used for comparing different results and assign goodness values based on their residuals. This method has been used for measuring improvements during the development.

We must emphasize that the proposed algorithms are distinct, they can be used in other applications together or separately since they are generally applicable, they do not depend on specialties of specific presented application.

Categories and Subject Descriptors

G.1.6 [Numerical Analysis]: Optimization; J.3 [Computing Applications]: Life and Medical Sciences

Keywords

digital angiography, parameter estimation

1 Problem addressed

The digital subtraction angiography [14] used in medical surgery is one kind of an image recording and processing method where panoramic x-ray images are taken while contrastive x-ray fluid [6] is injected into the patient's heart's main arteria. The goal is to estimate the probability of cardiac muscle regeneration of a patient who has recently survived a stroke, being dead blood cells removed by means of a surgery intervention. The x-ray fluid flow is similar to blood-flow [9], thus the amount of blood that can reach the critical region can be measured.

Given the images, the intensity of the x-ray fluid can be computed [2] by selecting the critical cardiac muscle region as the Region of Interest (ROI) [17] and calculating the average intensity of the pixels in it. In this way, we have an intensity value for each image which is going to be our initial sample ($M(t)$).

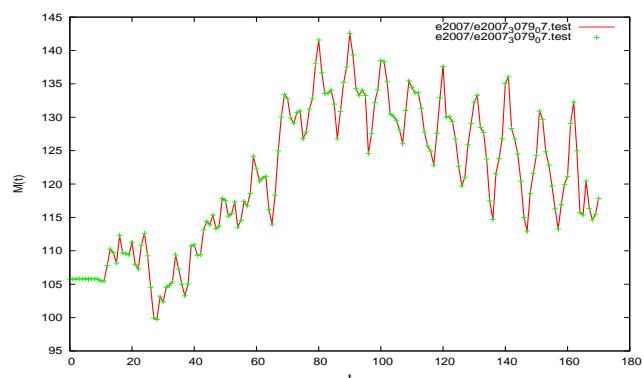


Figure 1. A typical initial intensity sample

1.1 Modelling flow dynamics

Our main task was to characterise the x-ray fluid flow in blood vessels by means of numerical values. To achieve this goal we had to pick a well-known and widely used [4] function which is appropriate for modelling flow dynamics. Our choice is the 5 parameter Gamma function [11] defined by

the equation

$$G(t) = \left\{ \begin{array}{l} Z_l \quad | \quad AT < t \\ K_s(t-AT)^\alpha e^{-\frac{-(t-AT)}{\beta}} + Z_l \quad | \quad AT \geq t \end{array} \right\},$$

where $K_s > 0$ is a scaling factor, $AT, Z_l > 0$ are offsets and $\alpha, \beta > 0$ are the rising and descending slope shape parameters.

In our application these values have biological meanings [11]. The AT parameter specifies the time when the contrastive fluid has been injected while Z_l and K_s are the base intensity and intensity scaling values of the x-ray device. The slope parameters describe the way blood can enter and exit the cardiac muscle in question, so our model can tell valuable information to surgeons.

Then, the objective was to efficiently fit this model to any kind of measurement with high confidence regarding the nature of the consequences our results could introduce. For this task we used the Levenberg-Marquardt method [12], [16], with a proper line-search minimizing the difference between the model and sample values in a nonlinear least squares way [5], [13]:

$$Z_{res} = \sum_{i=1}^n (G(t_i) - M(t_i))^2 \rightarrow \min. \quad (1)$$

1.2 Normalizing residual squares

To declare a fit good or bad, the sole sum of the residuals (Z_{res}) are not good enough, since a better fit can have higher Z_{res} values than a worse one because of heavy noise or badly scaled sample. Since Z_{res} can be of arbitrarily large, we propose a method for scaling these values into a properly chosen interval.

Let F be the vector of our fitted values, M the measurement vector, F_l, M_l lower and F_u, M_u upper bounds. Then $\forall i \in 1, \dots, n$

$$\begin{aligned} m_i &\in [M_l, M_u], & M_l &\leq M_u, & M_l, M_u &\in [0, 255], \\ f_i &\in [F_l, F_u], & F_l &\leq F_u, & F_l, F_u &\in [0, 255], \end{aligned}$$

and

$$(f_i - m_i) \in [F_l, F_u] - [M_l, M_u] = [F_l - M_u, F_u - M_l].$$

Now the natural interval extension of Z_{res} is:

$$\begin{aligned} Z_{res} &= \sum_{i=1}^n (F(t_i) - M(t_i))^2 \in \sum_{i=1}^n ([F_l - M_u, F_u - M_l])^2 \\ &\in \sum_{i=1}^n ([0, \max((F_l - M_u)^2, (F_u - M_l)^2)]) \\ &\in [0, n \max((F_l - M_u)^2, (F_u - M_l)^2)]. \end{aligned}$$

Since F_l, F_u, M_l, M_u values are computable, Z_{res} can be normalized:

$$\hat{Z}_{res} = \frac{Z_{res}}{n \max((F_l - M_u)^2, (F_u - M_l)^2)} \in [0, 1]. \quad (2)$$

2 Results on the initial samples

To evaluate our solution we had 66 real life, anonymous medical samples at our disposal. We must underline that these samples contain noises from different sources [8] (unprecise recording, unprecise fluid injection [6], [7] x-ray device's auto-intensity regulation, image processing bugs [15]) and our effort in figuring out suitable noise models was a fool's errand.

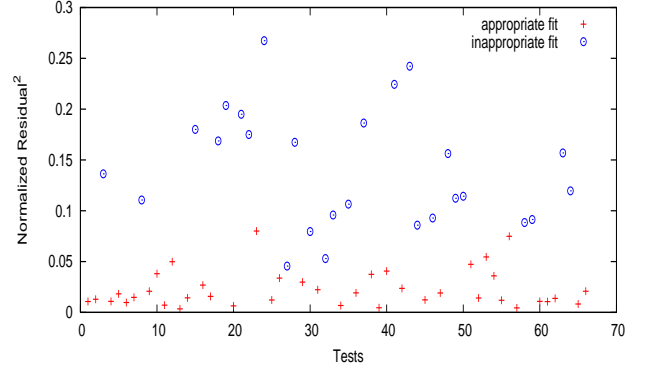


Figure 2. Normalized results on the test database

Our first results were generated by fitting our model on the raw samples with a constant initial guess vector $P_0 = (K_s, AT, \alpha, \beta, Z_l) = (0.02, 34.0, 3.3, 11.1, 106.0)$. Since the results were really bad (concerning either performance or precision), we classified each fit in a graphical way into *appropriate* and *inappropriate fit* classes (see Figure 2) and computed the normalized residuals. This is our control set for measuring the upcoming algorithm's improvements. On Figure 2 a somewhat sharp interface could be seen between bad and good fits meaning our normalization algorithm performs really well.

3 Noise filtering

In order to achieve better results, we have decided to apply a noise filtering algorithm whose primary goal was to eliminate spikes and produce a smoothed sample. Filters like median filters, arithmetic mean filters did not perform well on all types of measurements. The chosen filtering algorithm is a general Gaussian moving window average type [10] filter with specially designed weights and variable length window size. The weights are designed to be precomputable given an initial sample, and not to introduce undesired offsets and scaling on the input values:

$$M^*(t_i) = \sum_{j=i-L_w}^{i+L_w} \frac{M(t_j)}{2L_w + 1} w_j \quad \text{if } L_w \leq t_i \leq |M(t)| - L_w,$$

where $\forall j \in [i - L_w, i + L_w]$, and the weights are:

$$w_j = e^{-(t_j - t_i)^2 / (2L_w + 1)} \frac{2L_w + 1}{\sum_{j=i-L_w}^{i+L_w} e^{-(t_j - t_i)^2 / (2L_w + 1)}}. \quad (3)$$

By selecting the weights in this way, it is guaranteed that $\forall i \in [1, n]$:

$$\sum_{j=i-L_w}^{i+L_w} w_j = 2L_w + 1.$$

Generally speaking our proposed weighting method gives us a (not arithmetic) mean moving window filter with Gaussian weights.

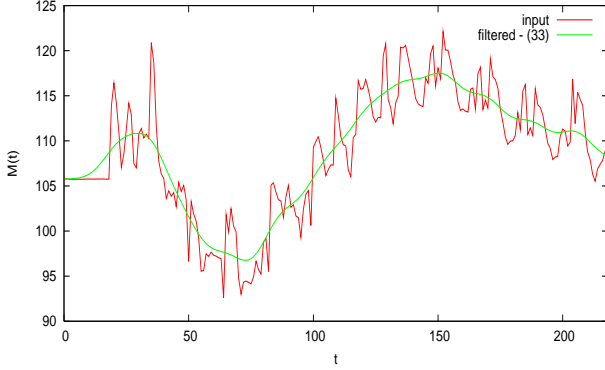


Figure 3. Filtering result with optimal window size

The second task was to determine a widely usable window size which eliminates local spikes but does not alters too much the initial sample's core. We have done an exhaustive search by computing the filtered sample $M^*(t)$ for each initial sample $M(t)$ with all possible usable window sizes (3 – 100). Then each filtered sample have been evaluated as good or bad resulting a histogram for appropriate window sizes having a maximum at 33.

Our proposed filtering algorithm can successfully be used on any one-dimensional sample since weights depend only on the measurement vector and the optimal window size can also be found in the above way.

3.1 Results on the filtered samples

When we modified the NLLS minimizer's objective function as to minimize the difference between the model and the **filtered sample**, significant improvements were achieved concerning the *precision*:

$\mathbf{M(t)}$	min	max	mean	median
iterations:	3	9999	3796.09	46
Z_{res} :	121.84	35815.86	7010.51	2811.72
CPU time (s):	0.01	7.22	2.03	0.21
$\mathbf{M^*(t)}$	min	max	mean	median
iterations:	4	9998	2158.71	45
Z_{res} :	122.09	30084.45	3730.36	2480.72
CPU time (s):	0.01	7.34	1.13	0.07

One can see that when using $M^*(t)$ as reference, on average approximately half the time is required to achieve double precision. When plotting the normalized residual values (Figure 4), the bad fit count decreased, also the interface between good and bad fit classes sharpened.

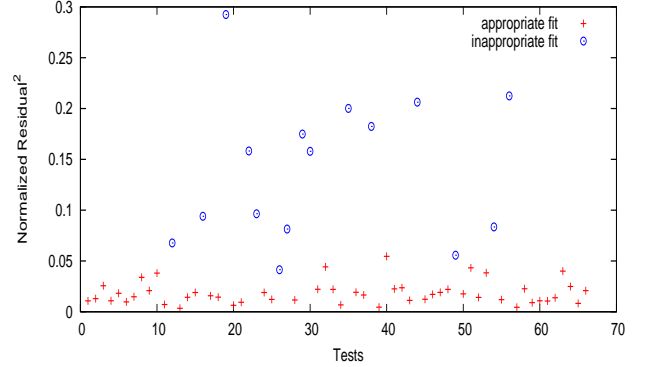


Figure 4. Normalized results on filtered samples

4 Initial guess computation

Given the nature of the source experiment (cardiovascular angiography), real solution vectors are expected to be scattered in the search space rather than in a certain cluster. Scattering means greater search space, which indicates that a static initial vector for the LM algorithm is in general a bad choice.

Now we propose an algorithm which is able to dynamically compute a really good approximation of the solution vector based on the filtered sample in $O(1)$ time and $O(n)$ space. This can also be used in other applications where our model is used.

It is known, that fluid injection is scheduled to be one second after the start of the recording, so the estimation of the Z_l parameter is trivial, we had to compute the arithmetical mean of the first 15 values of $M(t)$.

To estimate the other parameters, we have completed the functional analysis of the unscaled and unconditional model

$$H(t) = (t - AT)^\alpha e^{-\frac{t - AT}{\beta}} + Z, \quad (4)$$

computed the first order $H'(t)$ and second order $H''(t)$ derivatives and solved the $H'(t) = 0$ and $H''(t) = 0$ equations for identifying minimizer, maximizer and inflection points. The results showed that H has only a single maximum point (at t_{max}), and two inflection points (at $t_{i,1}$ and $t_{i,2}$). The interesting part is that these points can be computed simply using the model parameters:

$$t_{max} = \alpha\beta + AT, \quad (5)$$

$$t_{i,1} = \alpha\beta - \sqrt{\alpha}\beta + AT, \quad (6)$$

$$t_{i,2} = \alpha\beta + \sqrt{\alpha}\beta + AT. \quad (7)$$

In this way, if we are able to produce a good estimation for t_{max} , $t_{i,1}$ and $t_{i,2}$, by solving the above nonlinear systems of equations we got good estimations for AT , α and β . However the solution of this NLP problem is hard, complex NLP solvers are likely to introduce further errors, that is why we have chosen a simpler and faster heuristic method. Taking the above three equations the following expressions can be

derived:

$$\alpha = \frac{(t_{max} - AT)^2}{(t_{max} - t_{i,1})^2} = \frac{(t_{max} - AT)^2}{(t_{i,2} - t_{max})^2}, \quad (8)$$

$$\beta = \frac{(t_{max} - t_{i,1})^2}{t_{max} - AT} = \frac{(t_{i,2} - t_{max})^2}{t_{max} - AT}. \quad (9)$$

Since the AT parameter – the starting time of the rising slope of the model – can easily be detected on the filtered sample, and given the t_{max} and one of the $t_{i,1}$ and $t_{i,2}$ values, α and β are quickly computable using the equations (8) and (9). The estimation of the AT parameter is done by combining zero and first order assumptions on the ideal model:

$$AT \approx \frac{1}{3} \max_t (M^*(t) = 0) + \frac{1}{3} \max_t (M^*(t) = Z) + \frac{1}{3} \min_t (M^*(t) > Z).$$

Last but not least, an estimation for the K_s parameter must be given. This scaling is determined by the maxima of H (equation 4) and G . Since

$$H(t_{max}) = (\alpha\beta)^\alpha e^{-\frac{\alpha\beta}{\beta}} + Z = (\alpha\beta)^\alpha e^{-\alpha} + Z,$$

an approximation for K_s can be given by

$$K_s \approx \frac{\max(M^*(t)) - Z}{(\alpha\beta)^\alpha e^{-\alpha}}.$$

Figure 5 shows one output of our proposed algorithms in case of a quasi-bad measurement vector.

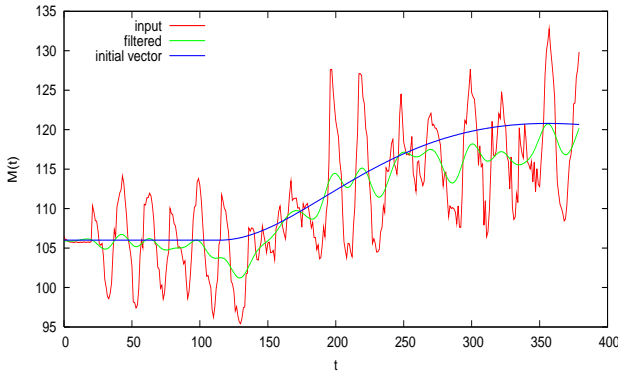


Figure 5. One result of the proposed algorithm

Our proposed algorithm performs really well, the initial guess that are computed could have been also accepted as the overall result of the fit! Using this algorithm, the residuals and the required time resources drastically decreased as compared to the previous approaches:

	min	max	mean	median
Z_{res} :	235.88	17085.28	4009.98	343.64
\hat{Z}_{res} :	0.0090	0.2379	0.0436	0.02719
CPU time(s):	0.01	0.26	0.025	0.02

Note that the above values are just the results of the initial guess computation algorithm, not the fit. When applying also

the LM algorithm and fed it with the pre-computed initial vector, more improvements has been achieved:

	min	max	mean	median
Z_{res} :	120.45	11245.8	3210.77	134.66
\hat{Z}_{res} :	0.007	0.231	0.0316	0.0187
CPU time(s):	0.01	2.54	0.42	0.05

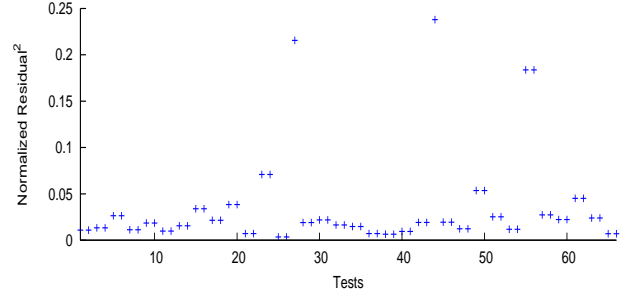


Figure 6. Normalized results with dynamic initial vector

On Figure 6 – showing the normalized residuals –, each fit has been classified as appropriate, the higher values indicate wrong samples which must be dropped or rerecorded. Figure 7 shows a bad measurement vector with its smoothed curve and the output of our algorithm which is a constant vector for every measurement of this kind.

We must note that our proposed algorithms have also been verified numerically to prove their correctness and usability. At this point, the required efficiency and precision has been achieved and having the verifications completed, the results can be trusted.

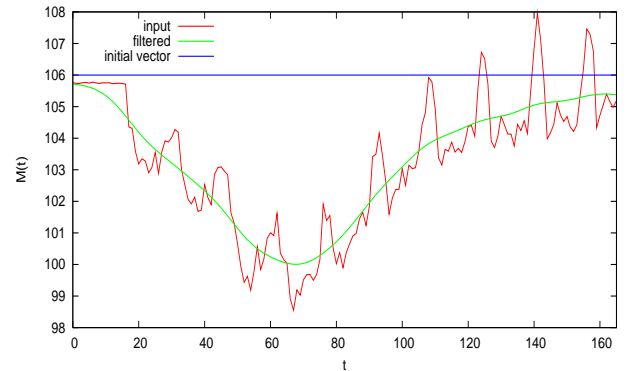


Figure 7. A typical wrong sample

5 Significant point selection

Furthermore, we wanted to compress the filtered sample [1], since an average of 200 values are too much for our model's 5 parameters [3]. Using less values (about 20), we expected that our fitting would be even more accurate and faster. The results showed a positive feedback.

Our basic idea was to classify the filtered sample's values as *significant* or *non-informational* points. To select the *significant* ones, we must detect those points where there are sudden changes in the $M^*(t)$ sample values. This is done

using its first order discrete derivative sample $\partial M^*(t)$ and dividing its codomain into a pre-defined number of intervals. Then, running through $\partial M^*(t)$ we track some history on the previously seen values and note those points where the previous point was located in another interval than the current one.

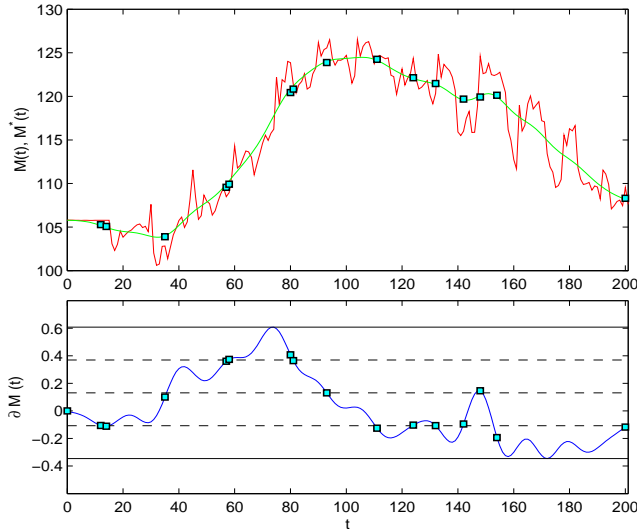


Figure 8. Significant point selection algorithm

The scheme of this method is shown on Figure 8, where the bottom graph shows the codomain of $\partial M^*(t)$ divided into 4 equidistant intervals. The blue squares are the selected *significant* points which are then projected onto the top graph. Also, special care was taken for avoiding multiple point selection around interval borders – when oscillation in the $\partial M^*(t)$ sample occurs.

Generally speaking, our algorithm approximates the curve with a polyline, and does its job really well (see Figures 9 and 10).

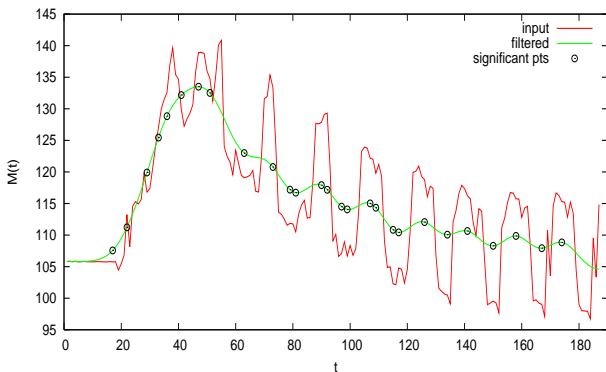


Figure 9. Significant point selection result number 1.

The proposed algorithm is designed to be driven by only one parameter – the *target significant point count* – and inside, everything is done to select as many points as requested, so more requested points mean more accurate approximation but less compression and vice versa.

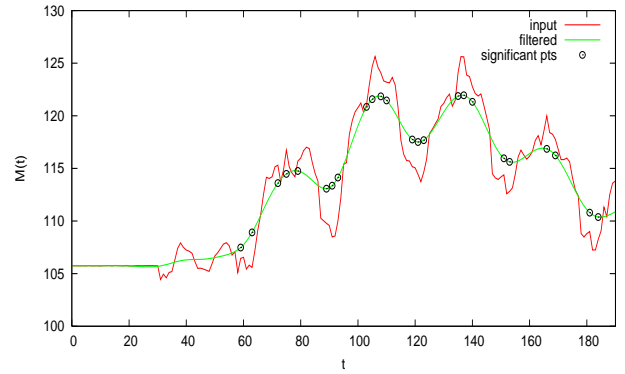


Figure 10. Significant point selection result number 2.

Take note that our third proposed algorithm can also be used on any kind of a discrete sample in any dimensions.

6 Final results

Finally, our complex solution consists of a special filter, a pure mathematical initial guess computation algorithm, a measurement compression method and last but not least a NLLS Levenberg-Marquardt solver. This is also the order of their application, so after getting the initial sample, we apply our filter, compute an appropriate initial vector and select significant points using the filtered sample, and apply the LM optimizer with the pre-computed vector and using only the significant data points in the objective function.

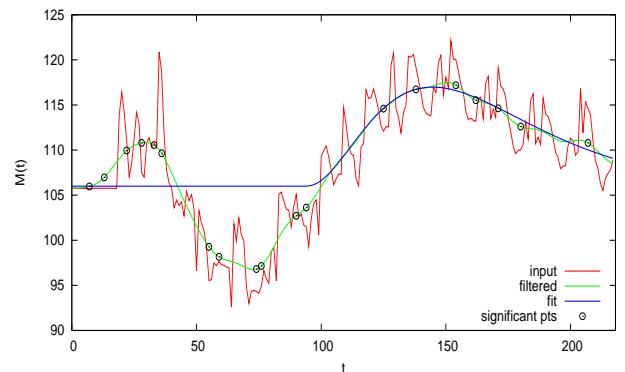


Figure 11. Composite result of a particular fit

Our composite solution technique is able to determine the validity of the measurement, then if it proves to be valid, we provide guaranteed results on any kind of input sample with high precision using no more than 2 seconds of computation time¹!

Comparing our solution with the time requirements of arranging the patient into the examination room, recording the x-ray video, image processing and ROI selection, we can surely say that our solution is really efficient and also effective enough to incorporate it into real-world devices.

¹Using an Intel Core 2 T2300, 4 GB RAM based PC

7 References

- [1] S. M. Ahmedaa and M. Abo-Zahhad. A new hybrid algorithm for ecg signal compression based on the wavelet transformation of the linearly predicted error. *Medical Engineering and Physics*, 23:117–126, 2001.
- [2] L. G. Brown. A survey of image registration techniques. *ACM Computing Surveys*, 24:325–376, 1992.
- [3] P. de Graaf, J. v. Goudoever, and K. Wesseling. Compressed storage of arterial pressure waveforms by selection of significant points. *Medical and Biological Engineering and Computing*, 35:510–515, 1997.
- [4] Y. Deuerling-Zheng, J. Boese, S. Achenbach, and J. Ludwig. Angiographic assessment of myocardial perfusion using correlation analysis. In *Bildverarbeitung für die Medizin 2007*, Informatik aktuell, pages 409–413. 2007.
- [5] M. Ghogho, A. Swami, and K. Asoke. Non-linear least squares estimation for harmonics in multiplicative and additive noise. In *Signal Processing*, pages 43–60, 1999.
- [6] C. Gibson, M. Anshelevich, and S. Murphy. Impact of injections during diagnostic coronary angiography on coronary patency in the setting of acute myocardial infarction from the timi trials. *Am J Cardiol.*, 86(12):1378–1379, 2000.
- [7] C. Gibson, A. Kirtane, and S. Murphy. Impact of contrast agent type (ionic versus non-ionic) used for coronary angiography on angiographic, electrocardiographic and clinical outcomes following thrombolytic administration in acute mi. *Catheter Cardiovasc Interv.*, 53:6–11, 2001.
- [8] C. Gibson and A. Schmig. Coronary and myocardial angiography: angiographic assessment of both epicardial and myocardial perfusion. *Circulation*, 109(25):3096–3105, 2004.
- [9] G. T. Gobbel, D. Christopher, E. Cann, and R. Fike John. 768 measurement of regional cerebral blood flow using ultrafast computed tomography theoretical aspects.
- [10] R. Haddad and A. Akansu. A class of fast gaussian binomial filters for speech and image processing. *IEEE Transactions on Acoustics, Speech and Signal Processing*, 39:723–727, 1991.
- [11] J. Howard K. Thompson, C. Frank Starmer, R. E. Whalen, and H. D. McIntosh. Indicator transit time considered as a gamma variate. *Circulation Research, American Heart Association*, 15:502–515, 1964.
- [12] M. I. A. Lourakis and A. A. Argyros. Is levenberg-marquardt the most efficient optimization algorithm for implementing bundle adjustment?, 2005.
- [13] K. Madsen, H. Bruun, and O. T. Imm. Methods for non-linear least squares problems. Technical report, 2004.
- [14] E. Meijering, W. Niessen, and M. Viergever. Retrospective motion correction in digital subtraction angiography: A review. *IEEE Transactions on Medical Imaging*, 18:2–21, 1999.
- [15] E. Meijering, K. Zuiderveld, and M. Viergever. Image registration for digital subtraction angiography. *International Journal of Computer Vision*, 31:227–246, 1999. 10.1023/A:1008074100927.
- [16] J. J. Moré. The Levenberg-Marquardt algorithm: Implementation and theory. In G. A. Watson, editor, *Numerical Analysis*, pages 105–116. Springer, Berlin, 1977.
- [17] S. Schafer, P. B. Nol, A. M. Walczak, and K. R. Hoffmann. Filtered region of interest cone-beam rotational angiography. *Medical Physics*, 37:694–704, 2010.